A Journal of the Gesellschaft Deutscher Chemiker

Angewandte International Edition GDCh Chemie

www.angewandte.org

Accepted Article

Title: A Cisplatin-Selective Fluorescent Probe for Real-Time Monitoring of Mitochondrial Platinum Accumulation in Living Cells

Authors: Jun Xiang Ong, Hai Van Le, Violet Eng Yee Lee, and Wee Han Ang

To be cited as: *Angew. Chem. Int. Ed.* 10.1002/anie.202010951

Link to VoR: https://doi.org/10.1002/anie.202010951

WILEY-VCH

10.1002/anie.202010951

WILEY-VCH

COMMUNICATION

A Platinum-Selective Fluorescent Probe for Real-Time Monitoring of Cisplatin Accumulation in Mitochondria in Living Cells

Jun Xiang Ong,[a]† *Hai Van Le,*[a]† *Violet Eng Yee Lee,*[a, b] *and Wee Han Ang**[a, b]

Abstract: *Mitochondria have emerged as important target for cisplatin in cancer therapy. Apart from cisplatin, many Pt complexes based on various scaffolds have also been developed to target mitochondria. Yet cellular processing of cisplatin or these mitochondria-targeting Pt analogues remained unexplored, largely due to a lack of tools capable of probing these Pt drugs within an intracellular environment. Herein, we developed the first mitochondria-targeting fluorescent probe for real-time monitoring of Pt accumulation in mitochondria and applied it to investigate mitochondria as cellular targets for anticancer Pt drug candidates in biological systems. We uncovered two distinct pathways whereby they could be delivered to mitochondria after cell entry.*

Cisplatin (cDDP), together with second-generation platinum-based drugs carboplatin and oxaliplatin, are amongst the most effective chemotherapeutic agents for the treatment of testicular, ovarian, lung and colorectal cancers.[1] Despite its potency and widespread use in the clinic, there remains considerable gaps in the understanding of its mechanism of action. It is generally accepted that cDDP exerts its cytotoxic effect by forming interstrand and intrastrand crosslinks with nuclear DNA which inhibit replication and transcription events, triggering apoptosis. However, the high cytotoxicity of cDDP in enucleated cells raises the question of non-nuclear targets of Pt drugs.[2] Studies have also showed that cDDP can exert its cytotoxicity by targeting other subcellular organelles.[3] Indeed, apoptosis induced by direct interaction with mitochondria may account for a significant portion of its antiproliferative activity, with mitochondria DNA being the likely target.[4] Other studies showed that Pt^{IV} prodrugs designed to deliver cDDP directly to mitochondria promoted cancer cell death.[5] This had led to a resurgence of interest in diamine Pt complexes designed to target mitochondria.[6] Yet how cDDP or these mitochondria-targeting Pt analogues are being processed intracellularly remain unexplored. In order to determine the role of mitochondria as biological target for cDDP, we developed a strategy for monitoring of cDDP to mitochondria in living cells using fluorescence microscopy.

Exogenous Pt-selective fluorescent probes have emerged as effective tools for studying the cellular processing of Pt-based anticancer compounds in biological systems. These exogenous Pt-selective probes are advantageous over the direct conjugation of fluorophores to Pt drugs as modification of Pt complexes with such bulky organic groups can significantly alter their drug uptake characteristics and pharmacokinetics, rendering them different from the parent drugs.[7] New and co-workers reported a fluorescein-based probe linked to a dithiocarbamic acid moiety and a rhodamine-based probe incorporating phenyl isothiocyanate to study the metabolism of Pt^{II} drugs.[8] Our group developed several rhodamine-based fluorescent turn-on and ratiometric probes equipped with dithiocarbamates as recognition motifs to study the intracellular activation of Pt^{IV} carboxylate prodrug complexes.[9] Leung and co-workers also developed a BODIPY-based probe for fluorescence imaging of cDDP.[10] However, these probes lack organelle-targeting abilities and cannot be applied to study cDDP accumulation in mitochondria. Herein, we developed the first mitochondria-targeting fluorescent probe for cDDP to investigate the mitochondria as cellular targets for cDDP and its Pt^{IV} prodrug derivatives, as well as to study transport pathways for intracellular Pt delivery to mitochondria.

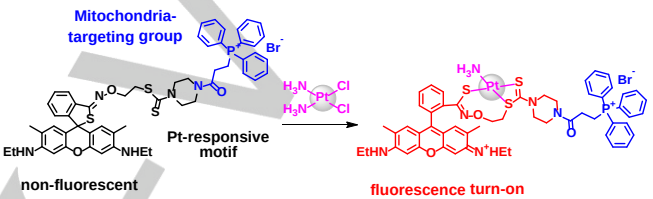

Figure 1*. Design of mitochondria-targeting probe* ***Rho-Mito*** *for organelle-specific monitoring of cDDP accumulation.*

In order to devise an efficient way of incorporating biological targeting groups onto the rhodamine-based fluorogenic scaffold, we developed rhodamine dithiocarbamate **2** (Scheme S1) as a precursor. This scaffold possessed the ability to bind to Pt^{II} species with its dithiocarbamate recognition motif while the free amine functional group enabled further synthetic modications. Therefore, amide conjugation with carboxylic acid derivatives of targeting groups enabled an efficent method to attach these targeting moieties onto the rhodamine fluorophore. The triphenylphosphonium (TPP) moiety was selected as a mitochondria-targeting functional group due to its chemical robustness and biocompatibility (Figure 1).[11] The resultant probe **Rho-Mito** responded to Pt^{II} species via a two-step binding mechanism culminating in spiro-ring opening.[9] The initial binding of dithiocarbamate to Pt^{II} complexes, including cDDP, resulted in the displacement of one of the chloride ligands. The thiocarbonyl group on the dithiocarbamate recognition motif labilised the *trans*-ligand via *trans*-effect, resulting in reaction with the spirothiophene on rhodamine and triggering spiro-ring opening. Rhodamine dithiocarbamate scaffold **2** was first prepared by reacting **1** with mono-piperazinyl dithiocarbamate. The reaction of **2** with 3-(triphenylphosphonium-propionic acid)bromide via amide coupling yielded **Rho-Mito** in moderate yields and fully characterized by NMR and ESI-MS.

We first explored the photophysical properties of **Rho-Mito** in the presence of Pt^{2+} metal ions. Titration experiment of **Rho-Mito** with K_2PtCl_4 was carried out in HEPES buffer (10 mM, pH 7.4, 30 % v/v EtOH). In the absence of Pt^{2+}, free probe presented only basal absorbance and fluorescence levels. When the probe was incubated with K_2PtCl_4 (0–15 equiv.), an absorption peak at 535 nm, typical of rhodamine 6G derivatives, was observed with intensities proportional to added Pt^{2+} ions (Figure S1). Similarly, stronger fluorescence emission bands at 565 nm were observed with gradual addition of K_2PtCl_4 (Figure S2). These observations could be attributed to spiro-ring opening of the spirothiophene after Pt^{2+}-binding, leading to fluorescence turn-on. Analysis of Job's plot indicated maximum

[a] Dr. J. X. Ong, H. V. Le, V. E. Y. Lee, Prof. Dr. W. H. Ang
Department of Chemistry, National University of Singapore, 3 Science Drive 3, Singapore 117543 (Singapore)
E-mail: ang.weehan@nus.edu.sg
[b] V. E. Y. Lee, Prof. Dr. W. H. Ang
NUS Graduate School of Integrative Sciences and Engineering Institution, National University of Singapore, 28 Medical Drive, Singapore 117456 (Singapore)
[†] These authors contributed equally to this work.

Supporting information for this article is given via a link at the end of the document.((Please delete this text if not appropriate))

10.1002/anie.202010951

WILEY-VCH

COMMUNICATION

Chart 1. *Molecular structures of* ***Rho-Mito*** *and Pt complexes.*

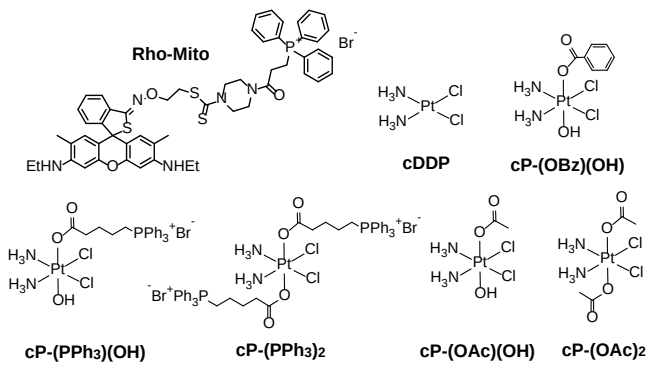

fluorescence intensity at a mole fraction of 0.5, which suggested that the probe interacted with Pt^{2+} in a 1:1 ratio (Figure S3). The free probe was stable over a wide pH range of 5–11 (Figure S4).

The excellent photometric response towards Pt^{2+} ions prompted us to apply **Rho-Mito** for the detection of Pt^{II} anticancer complexes including cDDP. Titration of **Rho-Mito** with cDDP (0–10 equiv.) also produced positive fluorogenic response, in keeping with previous Pt^{2+}-binding experiments (Figures 2a and S5). With the addition of increasing amounts of cDDP, emission intensity (I_{565}) of **Rho-Mito** displayed a strong linear correlation with cDDP concentrations from 0–100 μM. The detection limit (3σ/slope) for cDDP was determined to be 80 nM.[12] The selectivity towards cDDP was also high and competitive experiments showed that the presence of other biologically-relevant metal ions did not interfere with cDDP detection (Figure S6). Apart from cDDP, probe activation was also prominent against other promising Pt^{II} anticancer compounds such as JM118, picoplatin, carboplatin, pyriplatin and phenanthriplatin (Figures 2b and S7). However, Pt^{II} complexes containing chelating ammine ligands such as oxaliplatin and $Pt(en)Cl_2$ did not result in probe activation due to the inability of the dithiocarbamate recognition motif to displace the stable amine chelate.[9] In addition, **Rho-Mito** was also able to differentiate between Pt^{II} and Pt^{IV} metal complexes. Pt^{IV} complexes such as $cP\text{-}(OH)_2$, $cP\text{-}(OBz)_2$, $cP\text{-}(OAc)_2$ and satraplatin which are prodrug complexes based on either cDDP and JM118 did not result in probe activation. Since Pt^{IV} prodrug complexes undergo intracellular reduction to release active Pt^{II} species, **Rho-Mito** would be an ideal tool to study the accumulation and activation of Pt^{IV} prodrugs in the mitochondria.

The good sensitivity for cDDP together with its high selectivity and stability in physiological conditions indicated that **Rho-Mito** could be suitable for fluorescence imaging of cDDP in living cells. HeLa cells preincubated with **Rho-Mito** (10 μM) in culture medium for 30 min at 37 °C showed negligible fluorescence in the red channel (λ_{em}= 565 nm, Figure S8). When these pretreated cells were exposed to varying concentrations of cDDP at 1–10×IC_{50} concentrations, for 4 h, a significant increase in fluorescence intensities was observed that was dose-dependent. To examine the subcellular localization of **Rho-Mito**, we conducted colocalization experiments in HeLa cells by costaining **Rho-Mito** and commercial mitochondria tracker Rh 123 (λ_{ex}= 505 nm, λ_{em}= 530 nm). As shown in Figure 2c, fluorescence signals from the red channel attributed to **Rho-Mito** overlapped well with the green intracellular fluorescence of Rh 123 with a high Pearson's coefficient of 0.82 and overlap coefficient of 0.88 from the intensity correlation plot. The results demonstrated that **Rho-Mito** was mitochondria-targeted and could be applied as a turn-on probe for the detection of intracellular Pt^{II} anticancer complexes in living cells.

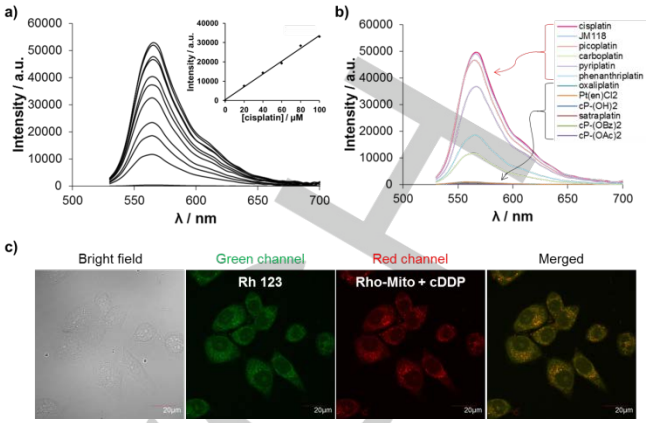

Figure 2. *(a) Fluorescence spectra of* ***Rho-Mito*** *(20 μM) titrated with cDDP (0–10 equiv.) in HEPES buffer (10 mM, pH 7.4, 30 % v/v EtOH) (λ_{ex}= 500 nm). Inset showing linear fitting curve of fluorescence intensity against cDDP (0–5 equiv.). (b) Fluorescence spectra of* ***Rho-Mito*** *(20 μM) after treatment with Pt^{II} and Pt^{IV} complexes (5 equiv.) in HEPES buffer (10 mM, pH 7.4, 30 % v/v EtOH) (λ_{ex}= 500 nm). Refer to SI for structures of Pt^{II} and Pt^{IV} complexes. (c) Fluorescence images of HeLa cells prestained with* ***Rho-Mito*** *(10 μM) treated with cDDP (30 μM), followed by incubation with commercial mitochondria tracker Rh123 (5 μM).*

If mitochondria were indeed important cellular targets of cDDP, changing its accumulation in mitochondria should directly affect its overall antiproliferative potency. To test this hypothesis, we proposed to knock down cellular transporters that trafficked cDDP into the mitochondria to effectively decrease mitochondrial cDDP levels. Cu transporters that regulate Cu homeostasis have been reported to facilitate the transportation of Pt-based anticancer drugs.[13] Cu influx transporter CTR1 membrane protein, Cu efflux transporters ATP7A and ATP7B have previously been shown to mediate the cellular uptake and efflux of cDDP, respectively. In particular, Cu chaperone COX17, associated with Cu transfer to mitochondria, was proposed to be involved in the transfer of cDDP to mitochondria. Using inductively coupled plasma mass spectrometry (ICP-MS) to quantify Pt levels in isolated mitochondria, Liu and co-workers demonstrated that transient knock down of COX17 resulted in lower mitochondrial cDDP levels and decreased potency.[14] However, elemental analytical methods such as ICP-MS can only perform end-point Pt determination, owing to their destructive nature, and not measurements in living cells required to study Pt accumulation over time. We therefore applied **Rho-Mito** for real-time monitoring of Pt accumulation in mitochondria of living cells to shed light on effects of transporter systems on cDDP trafficking.

Gene knockdown of COX17 in HeLa cells was carried out using commercial COX17 shRNA lentiviral particles which depleted intracellular COX17 expression in HeLa cells (COX17-KD). In contrast, viral transduction of control shRNA lentiviral particles had no effect on COX17 levels (control-KD, Figure S9). Cells were stained with **Rho-Mito** for 30 min, followed by treatment with cDDP for 4 h. Intracellular fluorescence intensities were determined using ImageJ software. The transduction of control shRNA into HeLa cells had no effect on the accumulation of cDDP in the mitochondria, as indicated by similar mean fluorescence intensities between control-KD and wild-type HeLa cells (Figure S10). In contrast, COX17-KD exhibited a 24 % decrease in fluorescence which suggested lower cDDP accumulation in the mitochondria. Mitochondrial Pt uptake measured by ICP-MS also showed 33 % decrease in Pt levels in COX17-KD cells, indicating that fluorescence data correlated well to the absolute Pt levels determined by ICP-MS

10.1002/anie.202010951

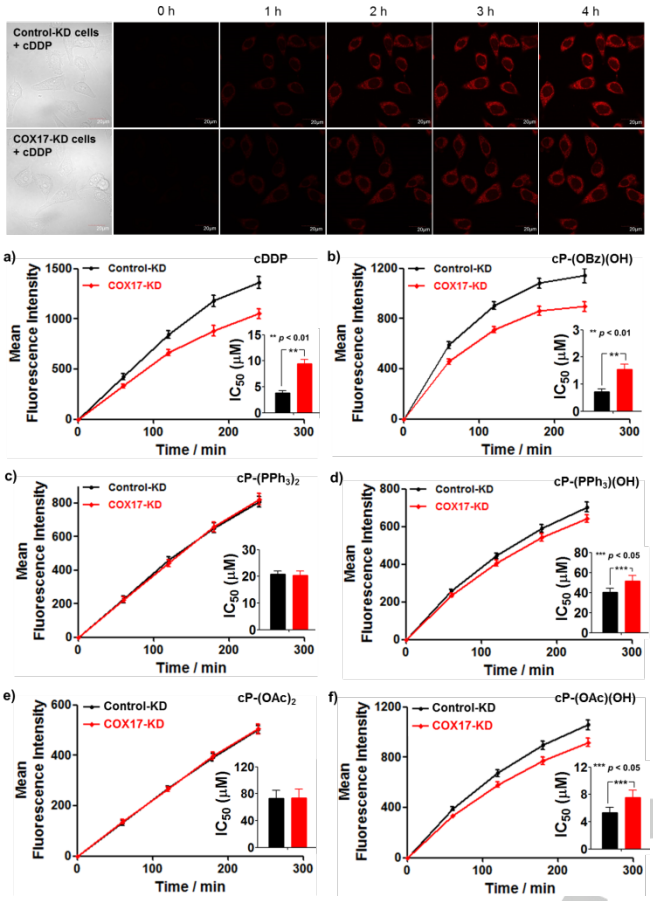

Figure 3. *(Top) Fluorescence images captured hourly over a period of 4 h of control-KD and COX17-KD HeLa cells prestained with* ***Rho-Mito*** *(10 μM) for 30 min, followed by treatment with cDDP (30 μM) at 37 °C; (Bottom) Graphs of mean fluorescence intensities calculated for every hour over a period of 4 h of control-KD and COX17-KD HeLa cells treated with (a) cDDP, (b) cP-(OBz)(OH), (c) cP-(PPh$_3$)$_2$, (d) cP-(PPh$_3$)(OH), (e) cP-(OAc)$_2$ and, (f) cP-(OAc)(OH).Insets showing IC$_{50}$ values of compounds in control-KD and COX17-KD HeLa cells.*

(Figure S11). Crucially, we were able to perform real-time monitoring of cDDP uptake in the mitochondria for the first time using **Rho-Mito**.

When we compared cDDP accumulation in control-KD and COX17-KD cells over a period of 4 h, we observed consistently lower cDDP uptake in COX17-KD cells (Figure 3, top). This decrease in cDDP accumulation as a direct consequence of reduced intracellular COX17 levels showed that COX17 was involved in cDDP transport to the mitochondria. Studies have suggested that binding of cDDP to recombinant COX17 produced predominantly mono-platinated COX17 adducts and the main binding site of cDDP to COX17 was proposed to be the Cu binding site in COX17.[14-15] These adducts facilitated delivery of cDDP to mitochondria which were subsequently released inside the mitochondria to exert its cytotoxic effect. The half maximal inhibitory concentrations (IC$_{50}$) for cDDP showed that downregulation of COX17 (COX17-KD vs control-KD) resulted in a 2.5-fold increase in the IC$_{50}$ values (Figure S12). The lower cDDP accumulation in the mitochondria contributed to a substantial decrease in the overall cytotoxicity of cDDP, implying that mitochondria were significant biological targets of cDDP.

Since direct binding of cDDP to COX17 was postulated to be requisite for mitochondrial transport, we investigated Pt^{IV} analogues cP-(PPh$_3$)$_2$ and cP-(PPh$_3$)(OH) that were based on cDDP pharmacophore but contained TPP targeting groups for passive mitochondrial uptake (Chart 1). The negative membrane potential of the inner mitochondrial membrane allowed drugs conjugated with the positively-charged TPP cation to diffuse across the mitochondrial membrane easily from the cytosol thereby permitting the drugs to accumulate selectively in mitochondria.[11] We hypothesized that both Pt^{IV} complexes were non-reactive towards COX17 by virtue of their kinetic inertness and would therefore bypass COX17-mediated transport mechanisms. Since **Rho-Mito** could differentiate between Pt^{II} and Pt^{IV} species in the mitochondria, we could determine the aggregated rate of delivery when cytotoxic Pt^{II} species were formed.

Real-time fluorescence imaging of cells treated with bisfunctionalised cP-(PPh$_3$)$_2$ showed a gradual increase in red fluorescence over a period of 4 h, indicating that cP-(PPh$_3$)$_2$ was reduced to active Pt^{II} species (Figure S13). As expected, the plot of mean fluorescence intensity against time showed that COX17-KD cells treated with cP-(PPh$_3$)$_2$ had no significant difference in Pt^{II} accumulation as compared to control-KD cells (Figure 3c) indicating that the Pt delivery was COX17-independent. However, when we investigated mono- functionalized cP-(PPh$_3$)(OH), we measured a 8 % decrease in Pt^{II} accumulation in COX17-KD compared to control-KD cells (Figures 3d and S14) which suggested mitochondrial transport was partly dependent on COX17. Indeed for cP-(PPh$_3$)$_2$, there were no significant differences in antiproliferative efficacies (IC$_{50}$ values) in control-KD and COX17-KD cells (Figure 3c). In contrast, cP-(PPh$_3$)(OH) was 1.3-fold less cytotoxic (Figure 3d) in COX17-KD compared to control-KD cells, in keeping with reduced mitochondrial Pt accumulation.

One explanation for this difference was that despite their inertness, Pt^{IV} complexes can be reduced upon cell entry to more reactive Pt^{II} species which could then harness COX17 for mitochondrial delivery. cP-(PPh$_3$)(OH) was endowed with a higher reduction potential due to the axial hydroxide ligand and more readily reduced than cP-(PPh$_3$)$_2$. This was consistent with earlier studies which showed that Pt^{IV} complexes with axial hydroxide ligands were readily reduced via an inner-sphere pathway through H-bonding networks.[16] To test this hypothesis, we investigated cP-(OBz)(OH), an analogous Pt^{IV} scaffold but with a non-targeting axial ligand (Chart 1).[17] COX17-KD cells treated with cP-(OBz)(OH) exhibited a 22 % decrease in Pt^{II} accumulation when compared to control-KD cells (Figures 3b and S15). Similarly, antiproliferative activity assay showed that cP-(OBz)(OH) was 2.1-fold less cytotoxic in COX17-KD compared to control-KD cells (Figure 3b) in keeping with the lower mitochondrial Pt accumulation. Considering both cP-(OBz)(OH) and cP-(PPh$_3$)(OH) were kinetically inert but more prone to reduction compared to cP-(PPh$_3$)$_2$, we surmised that they were reduced prior to mitochondrial delivery, which would account for differences in their responses to lowered intracellular COX17 levels. Similar trends were also observed in another pair of Pt^{IV} complexes, namely cP-(OAc)$_2$ and cP-(OAc)(OH). cP-(OAc)$_2$ also exhibited no significant differences in Pt^{II} accumulation and IC$_{50}$ values between control-KD and COX17-KD cells (Figures 3e and S16) whereas cP-(OAc)(OH), which would be more readily reduced, showed a 14 % decrease in Pt^{II} accumulation and was 1.4-fold less cytotoxic in COX17-KD cells (Figures 3f and S17).

Our findings suggested two distinct paths that can be exploited for intracellular mitochondrial Pt delivery. One path utilised mitochondrial chaperone proteins such as COX17 as shuttles to transport Pt to mitochondria. cDDP acted predominantly through this pathway via Pt-binding since COX17 knock down abrogated cDDP activity. The second path involved passive targeting of mitochondria using charged lipophilic ligands and therefore COX17-independent. In this pathway, cP-(PPh$_3$)$_2$ was preferentially accumulated in mitochondria by virtue of its TPP ligands which bypassed COX17-mediated delivery. Evidence for

this path was provided by matching mitochondrial uptake profiles of cP-$(PPh_3)_2$ regardless of COX17 status.

Earlier, Guo and coworkers observed that cP-$(PPh_3)_2$ exhibited stronger disruptive effect on mitochondrial morphology and function as compared to cDDP in cancer cells even though its cytotoxicity was inferior to that of cDDP.[5b] Our results corroborated this finding and suggested that cP-$(PPh_3)_2$ entered mitochondria intact and transported across the mitochondrial inner membrane by virtue of the large membrane potential.[18] Subsequent release of TPP ligands by reduction acted directly to disrupt mitochondrial metabolism by inhibiting electron transport chain.[19] cDDP, on the other hand, was previously shown not to affect mitochondrial respiration and metabolism,[20] while cP-(PPh_3)(OH) was partially reduced prior to mitochondrial entry resulting in the loss of TPP ligands. The lower cytotoxicity observed for cP-(PPh_3)(OH) compared to cP-$(PPh_3)_2$ indicated that mitochondrial disruption was more important as the determinant of efficacy given that both Pt^{IV} compounds exhibited similar Pt accumulation. In addition, the results suggested that in HeLa cells, the chaperone pathway represented the dominant Pt delivery path given its higher mitochondrial Pt accumulation levels for cDDP and cP-(OBz)(OH), resulting in more potent antiproliferative activities.

a)

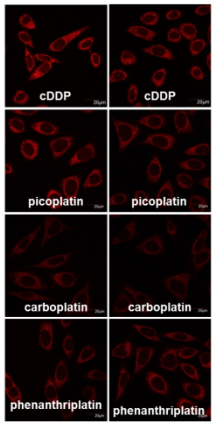

b)

Pt^{II} complexes	Mean fluorescence intensity[1]		
	Control-KD	COX17-KD	% decrease
cDDP	1346 ± 51	1022 ± 41	24
picoplatin	1176 ± 44	963 ± 39	18
carboplatin	618 ± 21	555 ± 16	10
phenanthriplatin	867 ± 35	865 ± 30	-

[1]Mean fluorescence intensities were measured with ImageJ software. In each experiment, at least five separate images from different regions of the glass slides were captured for mean fluorescence intensity calculations. All experiments were performed in triplicates.

c)

Pt^{II} complexes	IC_{50} [μM][2]		
	Control-KD	COX17-KD	Fold change
cDDP	4.01 ± 0.35	9.92 ± 0.75	2.5
picoplatin	4.68 ± 0.53	8.11 ± 1.12	1.7
carboplatin	12.26 ± 1.36	16.56 ± 2.17	1.3
phenanthriplatin	0.25 ± 0.05	0.22 ± 0.07	-

[2]Data obtained are based on the average of at least three independent trials, and the reported errors are the corresponding standard deviations. The IC_{50} were corrected using actual [Pt] determined using ICP-OES.

Figure 4. *(a) Fluorescence images of control-KD and COX17-KD HeLa cells prestained with* ***Rho-Mito*** *(10 μM) for 30 min, followed by treatment with different Pt^{II} complexes (30 μM) for 4 h at 37 °C. (b) Table of mean fluorescence intensities calculated for control-KD and COX17-KD HeLa cells after treatment with different Pt^{II} complexes for 4h. (c) Table of IC_{50} values of different Pt^{II} complexes in control-KD and COX17-KD HeLa cells.*

Apart from cDDP and its Pt^{IV} prodrugs, Pt^{II} complexes such as picoplatin and carboplatin were also observed to be taken up via the COX17-mediated pathway. Both picoplatin and carboplatin exhibited 18 % and 10 % decrease in Pt^{II} accumulation in COX17-KD cells, respectively (Figures 4 and S18). Similarly, the lower mitochondrial Pt accumulation resulted in picoplatin and carboplatin being 1.7-fold and 1.3-fold less cytotoxic in COX17-KD compared to control-KD cells, respectively (Figures 4c and S19). We postulated that the smaller decrease in mitochondrial Pt accumulation observed for carboplatin compared to cDDP in COX17-KD cells could be attributed to carboplatin being less reactive towards COX17-KD by virtue of its stable CBDCA chelate and was consequently less COX17-dependent. We further investigated phenanthriplatin which differs from cDDP by the presence of a phenanthridine ligand instead of a chloride in its structure. We hypothesized that the bulky phenanthridine ligand would make phenanthriplatin non-reactive towards COX17 and consequently COX17-independent. As expected, COX17-KD and control-KD cells treated with phenanthriplatin showed no significant differences in Pt^{II} accumulation as well as IC_{50} values (Figure 4). These results substantiated our earlier hypothesis that Pt complexes that are non-reactive towards COX17 would bypass COX17-mediated transport mechanisms.

In summary, we developed the first mitochondria-targeting fluorescent probe for real-time monitoring of cDDP accumulation in mitochondria. We showed that COX17 mediated the delivery of cDDP to mitochondria based on the evidence that cDDP accumulation in mitochondria was remarkably reduced in COX17-depleted cells. The decreased in cDDP levels in mitochondria also significantly reduced the overall potency of cDDP which indicated mitochondria to be important targets of cDDP in biological systems. We were also able to apply **Rho-Mito** to monitor real-time activation of Pt^{IV} prodrugs of cDDP as well as other Pt^{II} analogues. Unlike cDDP, the delivery of Pt^{IV} prodrugs of cDDP to mitochondria would not be mediated by COX17 due to their kinetic inertness except in instances when they are rapidly converted to cDDP. The use of passive targeting strategies can also potentially allow these Pt^{IV} prodrugs to bypass the COX17-mediated pathway but such strategies would require them to be stable in the presence of intracellular reductants. Structural modifications to the cDDP scaffold can directly affect COX17-binding, hence affect their transport via COX17-mediated pathways.

Acknowledgements

The authors gratefully acknowledge financial support from Ministry of Education and the National University of Singapore (R143-000-A66-112) as well as funding from the USyd-NUS Partnership Collaboration Award 2019.

Conflict of interest

The authors declare no conflict of interest.

Keywords: Cisplatin • Fluorescent probes • Mitochondria • Platinum drugs • Prodrugs

[1] a) D. Wang, S. J. Lippard, *Nat. Rev. Drug Discov.* **2005**, *4*, 307-320; b) L. Kelland, *Nat. Rev. Cancer* **2007**, *7*, 573-584.

[2] L. Galluzzi, L. Senovilla, I. Vitale, J. Michels, I. Martins, O. Kepp, M. Castedo, G. Kroemer, *Oncogene* **2011**, *31*, 1869-1883.

[3] S. M. Sancho-Martínez, L. Prieto-García, M. Prieto, J. M. López-Novoa, F. J. López-Hernández, *Pharmacol. Ther.* **2012**, *136*, 35-55.

[4] a) K. J. Cullen, Z. Yang, L. Schumaker, Z. Guo, *J. Bioenerg. Biomembr.* **2007**, *39*, 43-50; b) F. Gustavo, I. L. Clara, M. Jordi, *Curr. Pharm. Des.* **2011**, *17*, 2002-2016; c) X. Shu, X. Xiong, J. Song, C. He, C. Yi, *Angew. Chem. Int. Ed.* **2016**, *55*, 14246-14249.

[5] a) S. Marrache, R. K. Pathak, S. Dhar, *Proc. Natl. Acad. Sci. U.S.A.* **2014**, *111*, 10444-10449; b) S. Jin, Y. Hao, Z. Zhu, N. Muhammad, Z. Zhang, K. Wang, Y. Guo, Z. Guo, X. Wang, *Inorg. Chem.* **2018**, *57*, 11135-11145; c) M. V. Babak, Y. Zhi, B. Czarny, T. B. Toh, L. Hooi, E. K.-H. Chow, W. H. Ang, D. Gibson, G. Pastorin, *Angew. Chem. Int. Ed.* **2019**, *58*, 8109-8114.

[6] a) Simon P. Wisnovsky, Justin J. Wilson, Robert J. Radford, Mark P. Pereira, Maria R. Chan, Rebecca R. Laposa, Stephen J. Lippard, Shana O. Kelley, *Chem. Biol.* **2013**, *20*, 1323-1328; b) J. Li, X. He, Y. Zou, D. Chen, L. Yang, J. Rao, H. Chen, M. C. W. Chan, L. Li, Z. Guo, L. W. Zhang, C. Chen, *Metallomics* **2017**, *9*, 726-733; c) K. Wang, C. Zhu, Y. He, Z.

Zhang, W. Zhou, N. Muhammad, Y. Guo, X. Wang, Z. Guo, *Angew. Chem. Int. Ed.* **2019**, *58*, 4638-4643; d) Z. Zhu, Z. Wang, C. Zhang, Y. Wang, H. Zhang, Z. Gan, Z. Guo, X. Wang, *Chem. Sci.* **2019**, *10*, 3089-3095.

[7] a) S. Wu, X. Wang, C. Zhu, Y. Song, J. Wang, Y. Li, Z. Guo, *Dalton Trans.* **2011**, *40*, 10376-10382; b) S. Wu, C. Zhu, C. Zhang, Z. Yu, W. He, Y. He, Y. Li, J. Wang, Z. Guo, *Inorg. Chem.* **2011**, *50*, 11847-11849.

[8] a) C. Shen, B. D. Harris, L. J. Dawson, K. A. Charles, T. W. Hambley, E. J. New, *Chem. Commun.* **2015**, *51*, 6312-6314; b) J. L. Kolanowski, L. J. Dawson, L. Mitchell, Z. Lim, M. E. Graziotto, W. K. Filipek, T. W. Hambley, E. J. New, *Sens. Actuators B Chem.* **2018**, *255*, 2721-2724.

[9] a) D. Montagner, S. Q. Yap, W. H. Ang, *Angew. Chem. Int. Ed.* **2013**, *52*, 11785-11789; b) J. X. Ong, J. Y. Yap, S. Q. Yap, W. H. Ang, *J. Inorg. Biochem.* **2015**, *153*, 272-278; c) J. X. Ong, C. S. Q. Lim, H. V. Le, W. H. Ang, *Angew. Chem. Int. Ed.* **2019**, *58*, 164-167; d) J. X. Ong, W. H. Ang, *Chem. Asian J.* **2020**, *15*, 1449-1455.

[10] F.-K. Tang, J. Zhu, F. K.-W. Kong, M. Ng, Q. Bian, V. W.-W. Yam, A. K.-W. Tse, Y.-C. Tse, K. C.-F. Leung, *Chem. Commun.* **2020**, *56*, 2695-2698.

[11] J. Zielonka, J. Joseph, A. Sikora, M. Hardy, O. Ouari, J. Vasquez-Vivar, G. Cheng, M. Lopez, B. Kalyanaraman, *Chem. Rev.* **2017**, *117*, 10043-10120.

[12] B. Zhu, C. Gao, Y. Zhao, C. Liu, Y. Li, Q. Wei, Z. Ma, B. Du, X. Zhang, *Chem. Commun.* **2011**, *47*, 8656-8658.

[13] a) S. B. Howell, R. Safaei, C. A. Larson, M. J. Sailor, *Mol. Pharmacol.* **2010**, *77*, 887-894; b) R. Safaei, *Cancer Lett.* **2006**, *234*, 34-39.

[14] L. Zhao, Q. Cheng, Z. Wang, Z. Xi, D. Xu, Y. Liu, *Chem. Commun.* **2014**, *50*, 2667-2669.

[15] L. Li, W. Guo, K. Wu, Y. Zhao, Q. Luo, Q. Zhang, J. Liu, S. Xiong, F. Wang, *Rapid Commun. Mass Spectrom.* **2016**, *30*, 168-172.

[16] E. Dabbish, F. Ponte, N. Russo, E. Sicilia, *Inorg. Chem.* **2019**, *58*, 3851-3860.

[17] S. Q. Yap, C. F. Chin, A. H. H. Thng, Y. Y. Pang, H. K. Ho, W. H. Ang, *ChemMedChem* **2017**, *12*, 300-311.

[18] M. P. Murphy, *Biochim. Biophys. Acta Bioenerg.* **2008**, *1777*, 1028-1031.

[19] J. Trnka, M. Elkalaf, M. Anděl, *PLOS ONE* **2015**, *10*, e0121837.

[20] R. K. Pathak, R. Wen, N. Kolishetti, S. Dhar, *Mol. Cancer Ther.* **2017**, *16*, 625-636.

10.1002/anie.202010951

WILEY-VCH

Entry for the Table of Contents (Please choose one layout)

Layout 1:

COMMUNICATION

Real-time cisplatin trafficking: A mitochondria-targeting fluorescent probe was engineered to detect the clinically-important platinum drug cisplatin in real-time. The probe was applied to investigate the mitochondria as cellular targets for cisplatin and its analogues. Two distinct pathways whereby Pt complexes could be delivered to mitochondria after cell entry were uncovered.

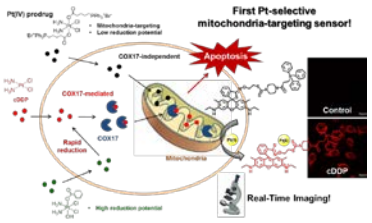

*Jun Xiang Ong, Hai Van Le, Violet Eng Yee Lee, and Wee Han Ang**

Page No. – Page No.

A Platinum-Selective Fluorescent Probe for Real-Time Monitoring of Cisplatin in Mitochondria in Living Cells

Layout 2:

COMMUNICATION

*Author(s), Corresponding Author(s)**

Page No. – Page No.

Title

Text for Table of Contents